Available online at www.sciencedirect.com
ScienceDirect
Sensors and Actuators B 122 (2007) 127–133
SENSORS AND ACTUATORS B CHEMICAL
www.elsevier.com/locate/snb

Less-mode optic fiber evanescent wave absorbing sensor: Parameter design for high sensitivity liquid detection

Yihui Wu [a,*], Xiaohong Deng [a,b], Feng Li [a,b], Xuye Zhuang [a,b]

[a] *National Key Laboratory of Applied Optics, Changchun Institute of Optics, Fine Mechanics and Physics, Chinese Academy of Sciences, Changchun, Jilin 130033, China*
[b] *Graduate School of Chinese Academy of Sciences, Beijing 100039, China*

Received 30 September 2005; received in revised form 16 May 2006; accepted 17 May 2006
Available online 27 June 2006

Abstract

This paper describes a theoretical way to design a fiber-optic evanescent wave sensor made by a partly unclad commercial optical fibers. The effects of the sensor's main parameters, such as absorbing medium refractive index, diameter of the fiber's bare core and the launching conditions, are analyzed theoretically. The differences of the radiation-field intensity in each optical mode are considered. The sensing region was obtained by HF etching with a silicon support. The prototype sensing devices were tested and partly explained by the calculation results. The methylene blue dye of 3.5×10^{-7} mol/L concentration was detected with the length of the sensing region of 14 mm. The bromcresol green in de-ionized water was measured in the experiment with 6.0×10^{-7} mol/L concentration.

Keywords: Optical fiber; Less-mode; Evanescent wave sensor; Sensitivity

1. Introduction

Evanescent wave fiber-optic absorption sensors have been successfully employed in studies of the solid–liquid interfaces, in chemical or biochemical reactions. The advantages of this method are its fast, real-time, in situ, remotely and safe detection. For application to micro biochemical systems, the high sensitivity and shorter length of the sensors are needed. There have been many efforts; for example, tapered [3], U-shaped [1], D-shaped [4] fiber-optic probe were fabricated for detection of several kinds of gases or liquids. There have been also theoretical evaluations for optimizing the structure parameters of the probes. Stewart et al. evaluated the attenuation of evanescent wave absorption by a ray-optics method, a perturbation method and a matrix method [5]. Gnewuch and Renner analyzed the power attenuation in multimode evanescent wave sensors by a perturbation method [6], and found that the waveguides with a linear refractive index profile showed mode-independent attenuation coefficients. Xu et al. [7] studied theoretically the contribution of the evanescent wave absorption with meridional and leaky skew rays, and found that the absorption models based only on meridional rays overestimated the absorption of the sensor. Qing et al. [9] proposed a group index method to evaluate the absorption coefficient of the optical waveguide chemical or biological sensors. In fact, as the dimension of the waveguide (or the core of fiber in this sensor) was usually in the same scale of its working wavelength, a doubt was raised whether the ray optics was still reasonable. Piraud et al. [8] studied the optoelectrochemical transduction of planar optical waveguides based on the electromagnetic field theory and wave optics. The effects on the modal absorption spectrum of a highly absorbing electrochromic film deposited on an optical waveguide were also modeled.

From the results of Qing [9], Wang [2] and our group [12], we knew that the sensitivity or absorption coefficient would be higher if the 0th mode or several modes exist only in the guiding film or core. That means it approaches to the single mode situation. In biochemical detection, however, the refractive indexes of liquid mediums to be detected are often around 1.33. In this situation the single mode condition is often satisfied when the diameter of the guiding core reaches several micrometers. Such an open-clad fiber-optic sensor makes the fabrication very dif-

* Corresponding author. Tel.: +86 4316176915; fax: +86 4315690271.
E-mail address: yihuiwu@ciomp.ac.cn (Y. Wu).

0925-4005/$ – see front matter © 2006 Elsevier B.V. All rights reserved.
doi:10.1016/j.snb.2006.05.026

ficult when commercial optic fibers are used. So, it is necessary to know whether the sensitivity could keep high with the same sensing length even if the number of modes is increased a little. In order to distinguish from normal multimode fiber evanescent sensors, we call it a less-mode optic-evanescent wave sensor.

In this paper the effects of the refractive index of the liquid medium, the core diameter of the sensing region and the modal fractional power in the liquid medium were studied based on the electromagnetic theory. The main differences from usual discussions are: (1) the calculation is not based on the assumption of the equally distributed power among modes and (2) the mode power in the unclad sensing region is discussed theoretically, while the light in the clad region is regarded as the source of this region.

Here the sensor was made by two kinds of commercial communication optical fibers (multimode and single-mode). The cladding diameters were both 125 μm, while the core diameters were 50 and 9 μm, respectively. The bare core was etched by HF to a designed diameter (several micrometers) and the sensing region was 14 mm in length. Then some of the theoretical results were compared with the experimental results.

2. Theory

It is well known that the guided light in a fiber-optic waveguide penetrates into the cladding to a distance of several wavelengths of the incident light as the evanescent tail of the waveguide mode. Suppose that the total modes of the optical fiber is N. For different modes the modal fractional optical power r_{fj} in the cladding and the modal percentage power in the total power η_j are all different. When α_m is defined as the bulk absorption coefficient, the total power transmitted through the uncladding part can be concluded by Lamber–Beer law as below.

$$P_{out} = \sum_{j=1}^{N} \eta_j P_{in} \exp(-r_{fj}\alpha_m CL) \tag{1}$$

where P_{out} and P_{in} are the power transmitted through the unclad region with and without an absorptive medium for sensing. C is the concentration of the absorptive medium. Then the sensitivity of the sensor will be

$$A_{EW} = \log_{10}\left(\frac{P_{in}}{P_{out}}\right) \tag{2}$$

And the total absorption coefficient can be written as $\gamma = a_m r_f$.

For a step-index optical fiber with charge free, homogeneous equations, the relationships between main parameters of the sensor were shown in a mode equation [10]. Here the transcendental equation was solved by the conditions of the mode cut-off and the continuation of electromagnetic fields at the boundary of absorptive and non-absorptive mediums. Suppose that the absorption of the optical fiber core is ignorable. Then the power fraction in the whole clad region is given by:

$$r_{fj} = \frac{p_2}{p_1 + p_2} = \frac{(1/2)\int_a^\infty \int_0^{2\pi} E_{r2} H_{\phi 2}^* r \,\mathrm{d}r \,\mathrm{d}\varphi}{(1/2)\int_0^a \int_0^{2\pi} E_{r1} H_{\phi 1}^* r \,\mathrm{d}r \,\mathrm{d}\phi + (1/2)\int_a^\infty \int_0^{2\pi} E_{r2} H_{\phi 2}^* r \,\mathrm{d}r \,\mathrm{d}\varphi} \tag{3}$$

and for TE modes

$$r_{fj} = \frac{p_2}{p_1 + p_2} = \frac{(1/2)\int_a^\infty \int_0^{2\pi} (-E_{\phi 2} H_{r2}^*) r \,\mathrm{d}r \,\mathrm{d}\phi}{(1/2)\int_0^a \int_0^{2\pi} (-E_{\phi 1} H_{r1}^*) r \,\mathrm{d}r \,\mathrm{d}\phi + (1/2)\int_a^\infty \int_0^{2\pi} (-E_{\phi 2} H_{r2}^*) r \,\mathrm{d}r \,\mathrm{d}\phi} \tag{4}$$

where the meaning of a, r and ϕ are shown in Fig. 1. The superscript "*" denotes complex conjugate, and other symbols have the conventional meanings.

2.1. The mode power percentage in the total power

If the incident light is a Gaussian beam and parallel with the fiber axis or has a slope angle θ_i, as shown in Fig. 1, the total power P of the beam in Z-direction can be expressed as

$$P = \pi n_i \left(\frac{\varepsilon_0}{\mu_0}\right)^{1/2} \rho_s^2 \tag{5}$$

where, ε_0 is the dielectric constant in vacuum, ρ_s is the radius of the light beam, μ_0 is the permeability in vacuum, n_i is the refractive index of air. In order to know the percentage of the power modes transmitted in the sensor's region, the total power launched in the optical fiber should be known first.

Here we suppose that the modes in the optical fiber are approximately orthonormal. The couple between modes was neglected even though the weak guiding conditions are not satisfied perfectly when the difference of the refractive index between the core and the detection medium is a little large. Considering the reflection on the launching side of the fiber, the power for mode exciting will be P'. The power transmitted in the jth mode is given by $P_j = |a_j|^2 N_j$ [11], where $N_j = (1/2)\left|\int A_\infty \vec{e}_{tj} \times \vec{h}_{tj}^* \times \vec{z}\,\mathrm{d}A\right|$ is the normalized factor, and a_j is

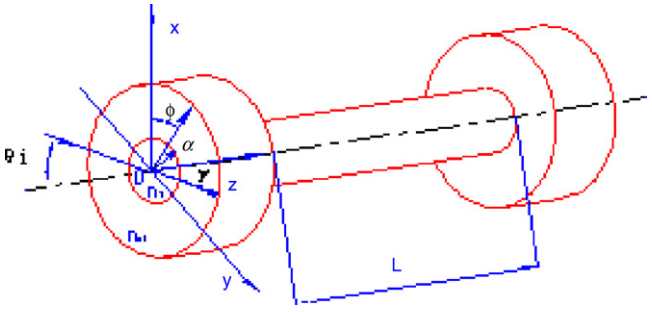

Fig. 1. Coordinate of beam field describing irradiation fiber end.

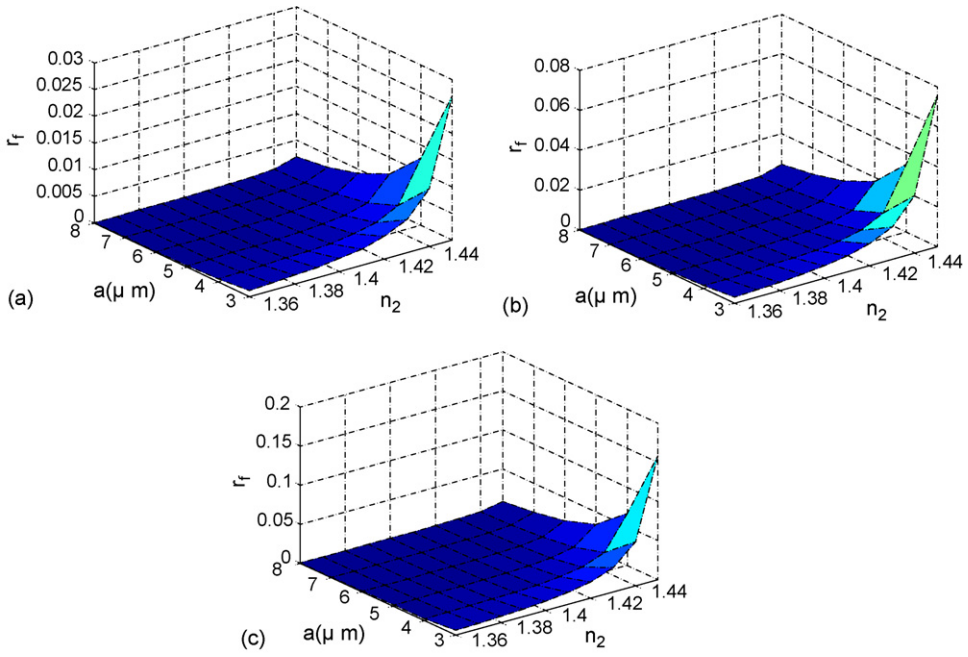

Fig. 2. Relationships among r_f and medium refractive index n_2, and sensing region radius a: (a) mode HE_{11}, (b) HE_{21}, and (c).

the amplitude of the mode. And the $\eta_j = P_j/P'$ is the mode power percentage in the total power.

For the sensing region, suppose that the number of modes is M, and the mode HE_{mn} will be excited in the sensing region with coefficient t_m. Then the percentage power of the guiding mode in the sensing region can be expressed as

$$\eta'_j = \frac{\sum_{K=1}^{N} \eta_j \times t_m}{\sum_{m=1}^{M}\sum_{n=1}^{N} \eta_j \times t_m} \tag{6}$$

2.2. Computational results and discussions

2.2.1. Mode fraction power in cladding

With an opened commercial optical fiber whose refractive index of the core is 1.468, the example curves of fraction power in the absorption medium are shown as a function of the core's radius a and the refractive index of the medium n_2 based on Eqs. (3) and (4) in Fig. 2. The wavelength of the source was chosen around the absorbing peak wavelength of the medium.

The examples in Fig. 2 show the examples how the absorption fraction power increases with increasing of the refractive index of the medium while decreases with increasing of the radium of the guiding core. Theoretically the value of r_f could be improved by increasing n_2 or decreasing a. When the normalized frequency is lower, r_f will be higher and more energy will be diffused in the medium. Because the absorptions coefficient γ is proportional to r_f, it is a way to improve the sensitivity.

2.2.2. Mode power percentage in the total power

From Eq. (6) the total power transmitted in the sensing region P_{bm} could be calculated. It is related with the radius of the light beam ρ_s and the slope angle θ_i. In order to simplified the calculation, the value of ρ_s was fixed at 4.3 μm, corresponding to the experiments with SMF-28 optical fiber. Here $\lambda = 632.8$ nm. The refractive index of the core is 1.468 and that of the clad is 1.465. Fig. 3 shows that for each mode the maximum coupling coefficients could be obtained by optimizing the slope angle θ_i. When θ_i gradually increases, the coupling coefficient of the fundamental mode and the coupling coefficients of higher order modes increase. Considering the signal to noise ratio, the slope angle θ_i should be smaller than θ_c. Here the complementary critical angle is 0.07 rad. When the polarization is in x-direction, there are HE_{11}, HE_{21}, HE_{31}, HE_{11} odd modes and TM_{01} modes. Because the number of guiding modes is effected by both n_2 and a, the power launched in optical fiber was discussed first.

The coupling coefficients of higher order modes are still larger when θ_i increases and approaches to θ_c. Cause in less-mode situation, the number of the high order modes will be more. This means that to increase the value of θ_i is a way to

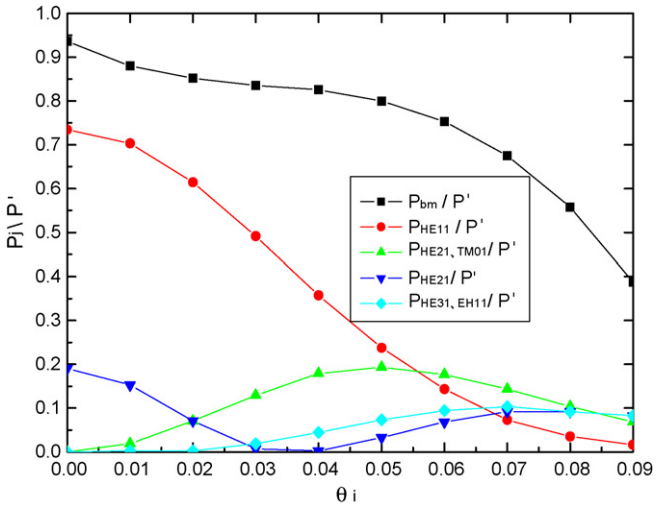

Fig. 3. The relation between P_j/P' and P_{bm}/P' with normalized slope angle θ_i.

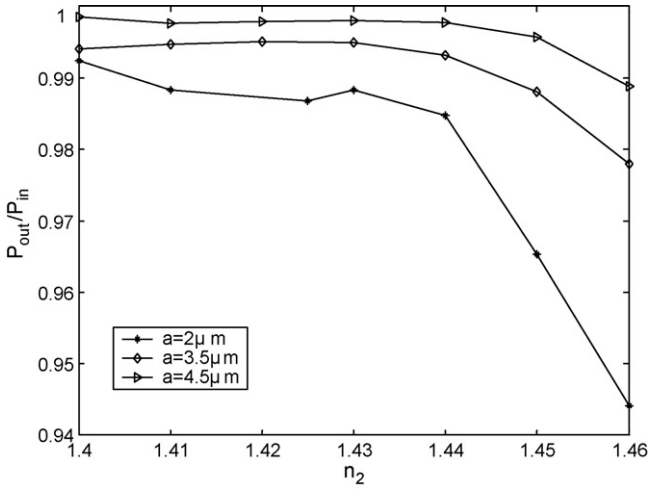

Fig. 4. The relationship between P_{out}/P_{in} and n_2 with different a.

increase the total transmitted power. So, the θ_i is fixed at θ_c in the discussions below.

2.2.3. Effects of a and n_2 to sensitivity

From Eqs. (1) and (6), the sensitivity for different a and n_2 can be obtained. Here $\rho_s = 2\,\mu m$, $\theta_i = \theta_c$, $n_1 = 1.4682$, $n_2 = 1.4646$, $L = 14$ mm, $L\alpha_m c = 0.3$.

Fig. 4 shows that when n_2 is selected to be approximately to n_1 (from 1.4 to 1.46), the P_{out}/P_{in} increases as a increases. That means the sensitivity becomes lower. With the same value of a, the P_{out}/P_{in} oscillating decreased as n_2 increased. The reason is when n_2 increased, r_{fj} increased, and at the same time the number of guiding modes decreased. But when n_2 is near the critical value for the mode number changing, the trend could be different, because when n_2 is a little smaller, the critical cut-off modes maybe exist, and these modes have rather big fraction powers. So the value of P_{out}/P_{in} will be smaller than the value when n_2 is a little bigger.

3. Experimental

3.1. Experimental setup

The experimental setup is shown in Fig. 5. The He–Ne laser used here was produced by Shanghai Aibo Laser Equipment Co., Ltd. (Type 260A, 632.8 nm). Its minimum output power was 1.8 mW, the maximum drift of it was ±3%, the beam diameter was 2 mm and the beam divergence is 1.5 mrad.

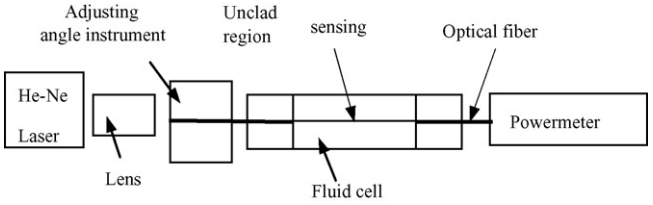

Fig. 5. The experimental setup.

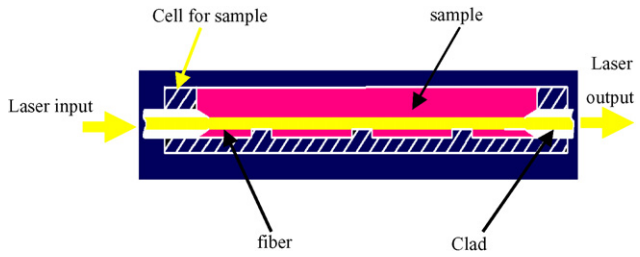

Fig. 6. The construction of the experimental.

As shown in Fig. 5, the laser was focused onto one end of the fiber, and the output power exported from the other end was measured by a commercial fiber-optic powermeter (PMS-2 made in China). The fiber-optic was mounted on a silicon support, as shown in Fig. 6.

The absorption medium used for experiments was methylene blue dye dissolved in de-ionized water and the absorbing peak was 664 nm. The concentration range of the methylene blue dye was from 2.5×10^{-6} to 3.5×10^{-7} mol/L. In this range the value of imaginary refractive index of the medium n_{2i} is much less than the real one, so that the effect of n_{2i} on propagation can be ignored. The real refractive indexes n_{2r} with different concentrations were measured by an Abbe Refractive Meter (model WAY, made in China) and showed that the differences were less than 0.05% in this range. Therefore, we regarded that the changes of P_{out} were mainly due to the differences of n_2.

3.2. Preparation of the sensing fiber

Different diameters of the sensing regions were fabricated by wet etching with the well know reactions:

$$4HF + SiO_2 \rightarrow SiF_4 + 2H_2O$$

$$6HF + SiO_2 \rightarrow H_2SiF_6 + 2H_2O$$

The velocity of etching is related to the concentration of HF. The main problem of this method is the risk of damaging the fiber when the fiber diameter reaches to several micrometers. As shown in Fig. 7, a powermeter was used to mon-

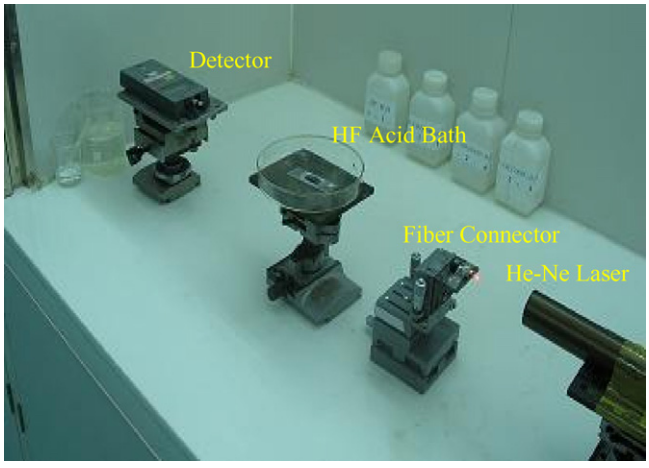

Fig. 7. The actual etching process.

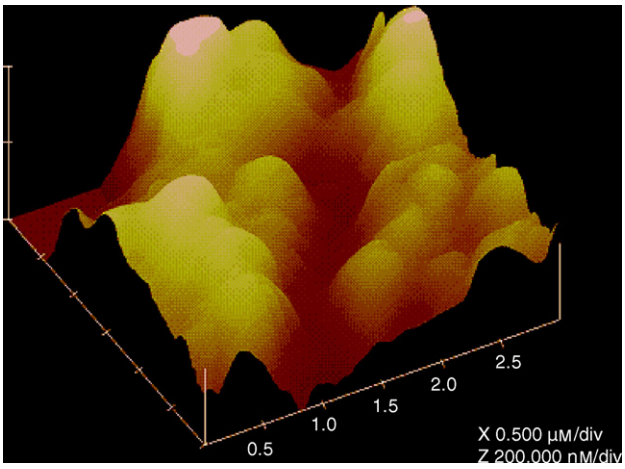

Fig. 8. The RFM photo of the fiber core surface etched by HF:H_2O (1:1).

itor the transmitted power which is a function of the core diameter.

Li [12] gave the relationship between the etching time and the fiber core diameter when H_2O:HF was 1:1. When the concentration of HF is high, the etching speed is high but the core surface is not perfect. By adding CH_3COOH as a buffer, the etching process becomes much more gently and the quality of the core surface becomes smooth, which is shown in Figs. 8 and 9.

After etching, because of the stress, the shape of the fiber will be changed so that it is difficult to do any operation. In order to solve this problem, we fixed the fiber first in the slot of the detection cell and then etched it. When the etching terminated, the core of the fiber was washed by de-ionized water and baked to release the remaining liquid. Then the detection cell with the fiber could be used as an evanescent wave sensor directly, as shown in Fig. 10.

3.3. Experimental results

Fig. 11 shows the experimental results on the relationship between the ratio P_{out}/P_{in} and n_2. In this experiment the sensor

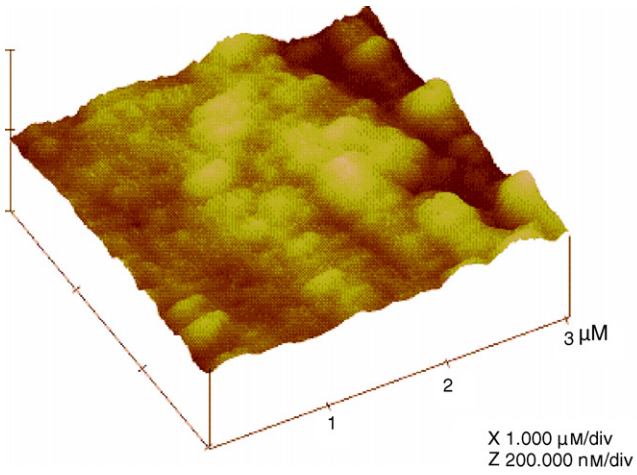

Fig. 9. The RFM photo of the fiber core surface etched by HF:CH_3COOH:H_2O (2:1:1).

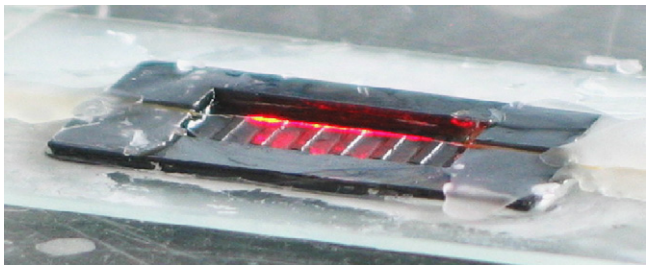

Fig. 10. The detection cell with the fiber.

was made by a multimode optical fiber (the core and cladding diameters were 50 and 125 μm, respectively). And the core refractive index was 1.485. The refractive index of the detection medium was adjusted by mixing glycerol in the medium with different ratios, and got the values from 1.335 to 1.445. The radius of the sensing part was 5 μm. It can be seen that the output power fraction reduced when n_2 increased. The trend with n_2 is similar to the results in Fig. 4. That means it is helpful to adjust the refractive index of the absorbing medium to meet the weakly guiding condition.

Fig. 12 shows the experimental and calculated value of P_{out}/P_{in} with the radius of the sensing part is 5 and 4.2 μm, respectively. Here, the refractive index n_2 of the absorbing medium was adjusted to 1.442 which was roughly met the weakly guiding condition, and the concentration of the medium was 1×10^{-5} mol/L. From the curves we can see the followings. (1) P_{out}/P_{in} reduces when θ_i increases. The experimental curve of $a = 5$ μm (single-mode) looks like a sine curve. It is because the optic fiber core (SMF-28) used was 9 μm. There was still a very thin cladding on it. We did also this experiment with another kind of optic fiber (MMF). The results are also shown in Fig. 12 (two 'multimode' curves). In this situation the difference is rather large. This is because the surface of the sensing fiber was poor, when the core diameter etched from 50 to 10 μm, and the taper at the two ends was also more obvious. (2) Both calculated and experimental results of P_{out}/P_{in} for the sensor with a core radius of 4.2 μm are less than those with a 5 μm core radius.

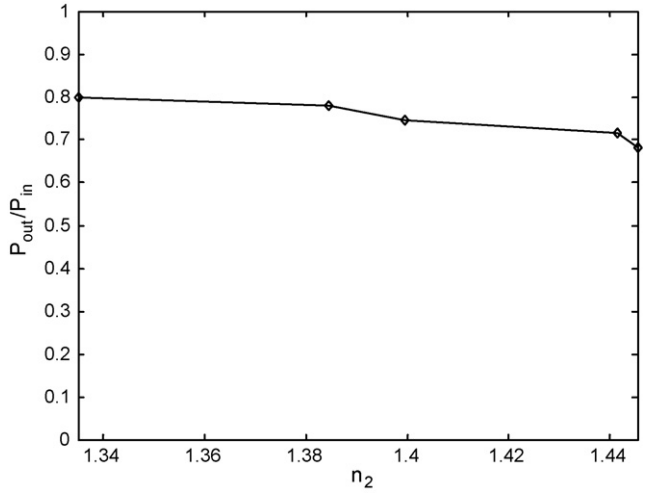

Fig. 11. The relationship between ratio P_{out}/P_{in} and n_2 from experiments.

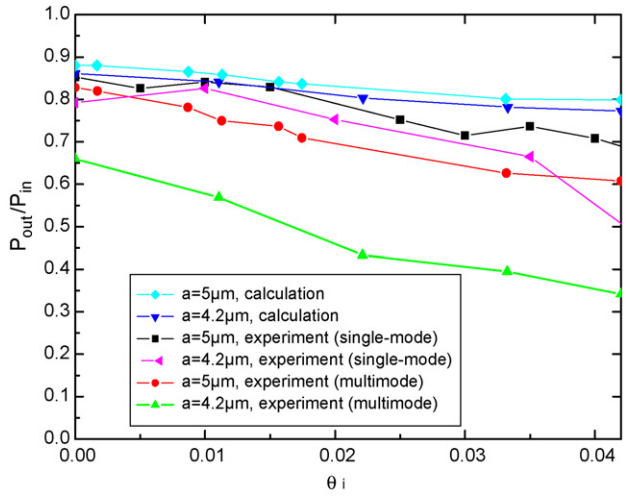

Fig. 12. Calculated and experimental values of P_{out}/P_{in} with the sensing region of a 5 and 4.2 μm radius.

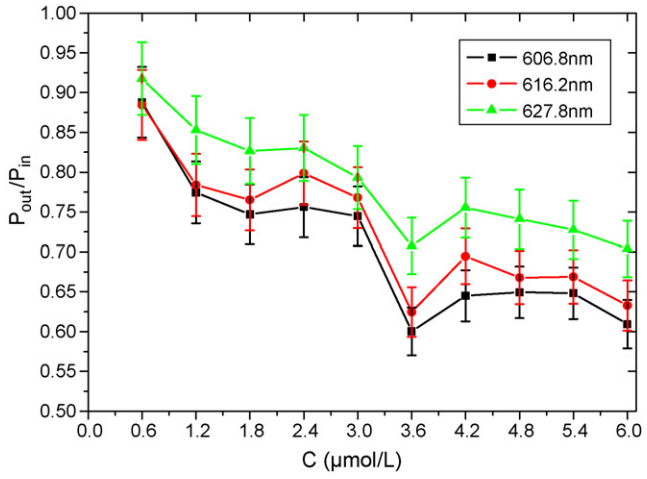

Fig. 14. The relationship between P_{out}/P_{in} and C of bromcresol green in de-ionized water with the sensing region of a 2.5 μm radius.

It is obvious that the experimental results are less than those of the calculation. The primary reason for this is that the scattering caused by the two tapered region, locating at the two ends of the sensing fiber, was not taken into account in the calculation, and also the scattering caused by the rough surface of the sensing fiber was neglected.

Fig. 13 shows the experimental results of the sensor made by SMF-28 optical fiber with a radius of 4.2 μm in the sensing region. The source was a He–Ne laser. In the experiments the concentration of methylene blue was from 3.5×10^{-7} to 2.5×10^{-6} mol/L. In this range the changes in refractive index was negligible.

Fig. 14 was the experimental results for the detections of bromcresol green in de-ionized water with a refractive index of 1.334. The change in refractive index was also neglected during the experiments. The sensor was made by SMF-28 optical fiber with a 2.5 μm sensing region radius. Because the absorption peak of bromcresol green is around 630 μm not 632.8 μm exactly, we chose a tungsten lamp (20 W, 12 V) in place of the He–Ne laser to get more precise results. The measured absorption spectra are shown in Fig. 15.

The results were for different concentrations and were read at three absorption wavelengths with a spectrometer made in our group and calibrated by LAMDA9. The lowest concentration here was about 6×10^{-7} mol/L. Because of the lower input coupling efficiency for this lamp the sensitivity was not very high.

From Fig. 15, we found that the absorption peak was shifted. It may be a function of the analyte concentration because of the hydrogen-bonding effects. Curves in Fig. 14 show deviations from Beer's law because of distortions of band profiles with variations in sample extinction coefficient. Other factors that affect Beer's law include surface contamination, mode-dependent attenuation and matching the numerical aperture (NA) of a fiber with light-coupling optics [15].

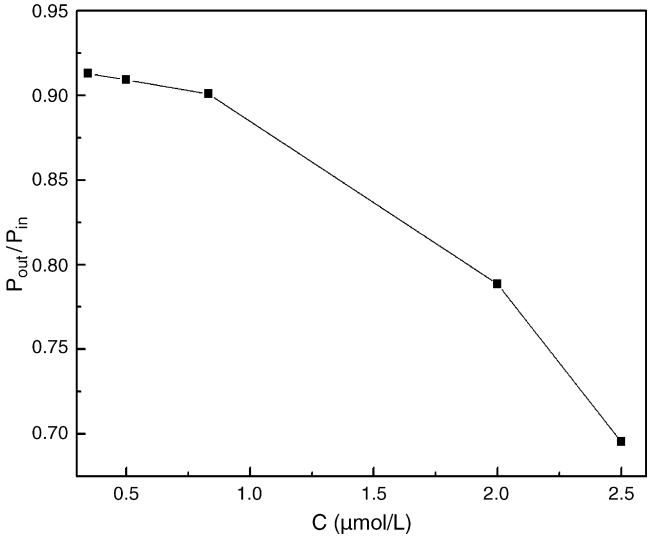

Fig. 13. The relationship between P_{out}/P_{in} and C of the methylene blue dye with the sensing region of a 4.2 μm radius.

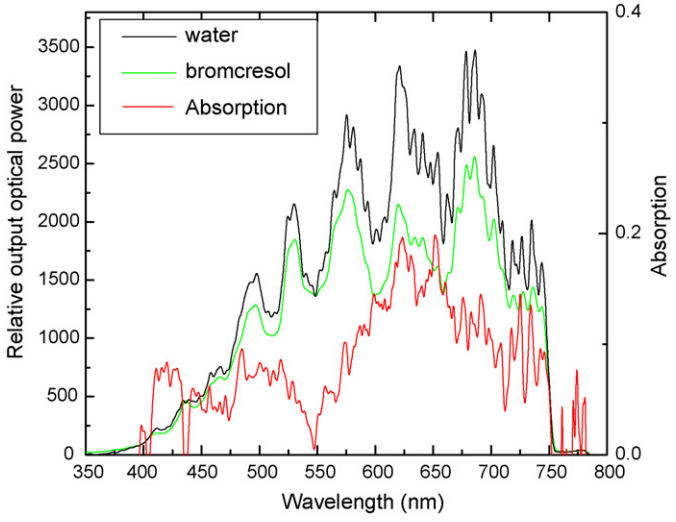

Fig. 15. The absorption spectra of bromcresol with the concentration 6×10^{-6} mol/L.

4. Discussions

The theoretical and experimental results all show that the sensitivity of the sensor is effected strongly by the parameters n_2, a and θ_i. In order to avoid too small diameter of the unclad sensing core, the refractive index of the detection medium should be increased to near to that of the core (here it is around 1.44). For this study we added the high index carrier (glycerine) in the detection liquid to see the influence of it. But in the real detection it could be rather complex with this carrier. In the continue study we will try to coat the right buffer layer on the unclad surface to instead of it. At the same time it is still possible to improve the fabrication processes to obtain the smooth unclad region of a smaller diameter. The mechanical way for a D-shape optical fiber sensor has been used, but in this way not all of the sensing part could be immersed in liquid samples. So the sensitivity may decrease for the same length of the sensing region. We started to make it by dry etching and fix it on the bottom of the cell. There is almost no risk of damage, but we should try to make the etching more efficient and low cost.

For different diameters of the sensing core, the θ_i should be different except that the single-mode conditions are satisfied. For a less-mode optic fiber changing the value of θ_i, the distribution of the power transmitted in models will be changed, the power transmitted in high-modes could be more and the effect of a could be compensated. Thus it is possible to get high sensitivity with a little bigger a.

The difference between the calculation and the experiments may come from the following factors: (1) the surface of the etched core is not perfect and scattering is obvious on the interface between liquid and solid, (2) the fiber diameter is unsymmetrical and there are errors in the measurement, and (3) the bending loss happens and increases the energy loss in the sensing region [1]. When the unclad optical fiber etched, taper will occur in the two ends of the sensing region. It is worth to mention that the fiber bend loss increases as its radius decreases. Various reasons have been assigned to this discrepancy [1]. A detailed theoretical explanation has been given by Payne and Hale [13]. Ruddy et al. mentioned that the non-linearity occurred due to the adsorption of the dye on the silica core surface [14], and this is not studied in this paper.

Acknowledgements

The authors acknowledge the supports from National Natural Science Foundation (60574089) and the National Key Lab of Applied Optics of China. The authors would like to thank Professor Jin Feng for his benefited discussions.

References

[1] B.D. Gupta, H. Dodeja, A.K. Tomar, Fiber-optic evanescent field absorption sensor based on a U-shaped probe, Opt. Quantum Electron. 28 (1996) 1629–1639.

[2] T.Y. Wang, et al., Analysis of evanescent wave transmission on single-mode optical fibers, J. Opto-electron Laser 14 (2003) 136–139.

[3] M. Ahmad, L.L. Hench, Effect of taper geometries and launch angle on evanescent wave penetration depth in optical fibers, Biosens. Bioelectron. 20 (2005) 1312–1319.

[4] B. Culshaw, F. Muhammad, G. Stewart, Evanescent wave methane detection using optical fibers, Electron. Lett. 28 (1992) 2232–2234.

[5] G. Stewart, B. Culshaw, Optical waveguide modeling and design for evanescent field chemical sensor, Opt. Quantum Electron 26 (1994) s249–s259.

[6] H. Gnewuch, H. Renner, Mode-independent attenuation in evanescent-field sensor, Appl. Opt. 34 (1995) 1473–1483.

[7] Y. Xu, A. Cottenden, N.B. Jones, A theoretical evaluation of the fiber-optic evanescent wave absorption in spectroscopy and sensors, Opt. Laser Eng. 44 (2006) 93–101.

[8] C. Piraud, E. Mwarania, J. Yao, K. O'Dwyer, D.J. Schiffin, J.S. Wilkinson, Optoelectrochemical transduction on planner optical waveguides, J. Lightwave Technol. 10 (1992) 693–699.

[9] D.-K. Qing, X.-M. Chen, K. Itoh, M. Murabayashi, A theoretical evaluation of the absorption coefficient of the optical waveguide chemical or biological sensors by group index method, J. Lightwave Technol. 14 (1996) 1907–1917.

[10] L.Y. Quan, C. Min, Optical waveguide theory and technique, P.P.T., Beijing, 2002, pp. 93–99.

[11] A.W. Snyder, J.D. Love, Optical waveguide theory, Chapman and Hall, New York, 1983, pp. 264–266.

[12] F. Li, Study on photometric absorbing spectral analysis in micro-fluidic chips, in: Master Paper of Chinese Academy of Sciences, 2004, pp. 30–32.

[13] F.P. Payne, Z.M. Hale, Deviation from Beer's Law in multimode optical fiber evanescent field sensor, Int. J. Optelectron. 8 (1993) 743–748.

[14] V. Ruddy, B.D. MacCraith, J.A. Murphy, Evanescent wave absorption spectroscopy using multimode fibers, J. Appl. Phys. 67 (1990) 6070–6074.

[15] R.A. Potyrailo, V.P. Ruddy, G.M. Hieftje, Kramers–Kronig analysis of molecular evanescent-wave absorption spectra obtained by multimode step-index optical fibers, Appl. Opt. 35 (1996) 22–26.

Biographies

Yihui Wu received her PhD in Engineering in Changchun Institute of Optics, Fine Mechanics and Physics (CIOMP), Chinese Academy of Sciences, Changchun, China, in 1996. She was a visiting scholar for 11 months in 2000 at the LMPO laboratory in France. She got research professor position in this institute since 1999. Her research interests are chemical and biological sensors, MEMS and spectro-analyse systems.

Xiaohong Deng received her BS from Xi'an Jiaotong University in 2003 and MS from Changchun Institute of Optics, Fine Mechanics and Physics, Chinese Academy of Science in 2006. Her main research field is optical fiber sensors.

Feng Li received his BS from Changchun University of Science and Technology in 2002 and MS from Changchun Institute of Optics, Fine Mechanics and Physics, Chinese Academy of Science in 2004. He is now preparing his PhD thesis on MEMS jointly in LMPO laboratory and Changchun Institute of Optics, Fine Mechanics and Physics.

Xuye Zhuang received his BS from Southwest Petroleum University, China, in 2004. Now he is preparing his MS thesis on MEMS in CIOMP.